ROS

RESEARCH ARTICLE

Brains from Aged *OPA1*$^{+/-}$ (B6;C3-Opa1 329-355del) Mouse Strain Are in a Pro-Oxidative State

Marlène Daloyau[1], Aurélie M.C. Millet[1], Marie-Christine Miquel[1], Valérie Mils[1], Bernd Wissinger[2], Pascale Belenguer[1], and Noélie Davezac[1]

[1]Research Center on Animal Cognition (CRCA), Center for Integrative Biology (CBI), Toulouse University, CNRS, UPS, France; [2] Centre for Ophthalmology, University of Tübingen, Roentgenweg 11, D-72076, Tübingen, Germany

Correspondence: noelie.davezac@univ-tlse3.fr (N.D.)

Daloyau M et al. Reactive Oxygen Species 6(18):396–405, 2018; ©2018 Cell Med Press
http://dx.doi.org/10.20455/ros.2018.863
(Received: June 26, 2018; Revised: July 12, 2018; Accepted: July 13, 2018)

ABSTRACT | Mutations in the OPA1 gene induce haploinsufficiency that instigates dominant optic atrophy (DOA), an incurable hereditary retinopathy with syndromic forms in up to 20% of patients, particularly affecting neurons. To identify the consequences of OPA1 loss of function on intracellular redox homeostasis, we used the DOA mouse model B6; C3-OPA1329-355del (*OPA*$^{+/-}$). Brain cortices from 15-month-old *OPA*$^{+/-}$ mice and littermates *OPA*$^{+/+}$ were analyzed for their aconitase activity and antioxidant defenses. We found a decreased aconitase activity testifying an increase in ROS levels together with constant levels of antioxidant enzymes quantities such as superoxide dismutase 1 (SOD1), SOD2, or catalase in 15-month old *OPA*$^{+/-}$ mice. Likewise, catalase activity is stable in the two genetic backgrounds. Interestingly, the pro-oxidative state that we identified in the brain tissues of 15-month-old DOA mice was previously observed in the 4- and 10-month-old DOA mice model. Thus, brain cortices from aged *Opa1*$^{+/-}$ mice are in a pro-oxidative state.

KEYWORDS | Aging; Antioxidant defenses; Mitochondria; OPA1; Optic atrophy; Oxidative stress

ABBREVIATIONS | DOA, dominant optic atrophy; LHON, Leber hereditary optic neuropathy; mtDNA, mitochondrial DNA; RGC, retinal ganglion cell; ROS, reactive oxygen species; SOD, superoxide dismutase

CONTENTS

1. INTRODUCTION

Mitochondria act as cellular powerhouses via oxidative phosphorylation [1] and mitochondrial diseases can be caused by mutations in the genes of mitochondrial or nuclear DNA [2]. Although many of these diseases are multisystemic, some are tissue-specific such as optic neuropathies that are due to alterations of mitochondrial functions [3], as illustrated by the identification of ND1–6, OPA1, OPA3, and TMEM126A as causative genes for Leber hereditary optic neuropathy (LHON) (OMIM#535000), type 1 autosomal dominant optic atrophy (OMIM#165500), autosomal dominant optic atrophy and cataract (OMIM#606580), and recessive optic atrophy 7 (OMIM#612989), respectively, to which numerous syndromic forms of optic atrophy implying mitochondrial proteins (FDRA, HSP7, and HMSN) are added up.

Dominant optic atrophy (DOA), also known as Kjer's disease, is characterized by moderate to severe loss of visual acuity, due to a loss of retinal ganglion cells (RGCs) whose axons form the optic nerve. Onset is insidious in early childhood and penetrance may be as low as 40% [4–6]. With an estimated disease prevalence of 1:10,000 in Denmark and 1:50,000 worldwide, this complex pathological condition remains without effective treatment. The majority of patients with DOA harbor mutations in the *OPA1* gene coding for a mitochondrial GTPase [7, 8]. To date, 280 different *OPA1* mutations have been reported (http:/mitodyn.org), the majority of which result in premature termination leading to haploinsufficiency by the reduction in OPA1 protein levels [4]. While the rate of disease progression displays a marked inter- and intra-familial variability, a significant proportion of patients (50–75%) will further experience visual worsening in life [9, 10]. Lastly, recent studies show a severe multi-systemic disorder associated with some *OPA1* mutations, named 'DOA plus' (DOA+) syndrome (OMIM#125250) [11–14]. These observations are of major pathophysiological importance, highlighting the widespread deleterious consequences of OPA1 mutations, not only for RGCs, but particularly for other neuronal populations, as well as skeletal and extra-ocular muscles [13, 15, 16]. These patients indeed present additional neurological complications and a 2–3-fold increased risk of developing multisystem neurological disease with missense *OPA1* mutations located within the GTPase domain, suggesting deleterious OPA1 loss-of-function mechanisms. Although these syndromic DOA variants show significant phenotypic variability, a consistent finding is a worse visual prognosis among this patients' subgroup.

The *OPA1* gene encodes the OPA1 mitochondrial protein partly localized in the mitochondrial intermembrane space (IMS) and anchored to the mitochondrial inner membrane [17–20]. Using common genetically modified cell lines (HeLa, COS, and MEF), we and others have shown that OPA1 has various functions [21], including inner membrane fusion, cristae structuration, mitochondrial DNA (mtDNA) maintenance, mitochondrial energetics modulation, and protection from apoptosis [21–24]. Skin fibroblasts, muscle cells, or lymphoblasts isolated from the patients have shown impairments in mitochondrial morphology, respiration and energetics, loss of mtDNA integrity, and an increased sensitivity to apoptosis [25, 26]. The DOA or DOA^{+} mouse models showed mitochondrial fragmentation, cristae disorganization, increased mitophagy, and cytochrome c oxidase deficiency [27–29]. Two DOA invertebrate models [30–33] emphasized a critical generation of ROS associated with OPA1 dysfunction, as it was proposed for (LHON) [34] and other neurodegenerative pathologies such as Alzheimer's and Parkinson's diseases [35]. We thus previously addressed the question of the general impact of OPA1 inactivation on oxidative metabolism in a DOA mouse model and demonstrated the implication of reactive oxygen species (ROS) as a key determinant of DOA pathogenesis in mammals at as early as 4 months of age [36]. Our results indeed showed that aconitase activity is inhibited in the brain cortices of 4- and 10-month-old *Opa1*$^{+/-}$ mice, underlying an increase in mitochondrial ROS production, together with elevated levels of superoxide dismutases (SODs) leading to a pro-oxidative state [36]. Since the symptoms of the disease worsen with age, we here addressed the question of the evolution of oxidative defenses in the

brain cortices of 15-month-old *Opa1*$^{+/-}$ mice. We found a decreased aconitase activity with no increase in antioxidant enzyme quantities such as SOD1, SOD2, and catalase. This demonstrated that 15-month-old DOA mouse brain cortices are still in a pro-oxidative state. Moreover, we found that the antioxidant defenses in the livers of 4- and 15-month-old DOA mice were not significantly different between genotypes regardless of age (data not shown).

2. MATERIALS AND METHODS

2.1. *Opa1*$^{+/-}$ and *Opa1*$^{+/+}$ Mice

Mice were housed in groups of five, kept in a specific pathogen-free and temperature-controlled facility, in a 12 h light/12 h dark cycle with food and water available ad libitum in full-barrier facilities free of specific pathogens. Mouse breeding and all experimental procedures were performed according to ethical laws of CNRS (Centre National de la Recherche Scientifique) and FRBT (Fédération de Recherche en Biologie de Toulouse). The animal facility called Genotoul Anexplo is maintained in accordance to F.E.L.A.S.A organism (Federation of European Laboratory Animal Science Associations). Two sanitary controls are done per year following the set point CO66. The B6;C3-*Opa1*$^{329\text{-}355del}$ mouse strain (abbreviated *Opa1*$^{+/-}$ mouse) has been previously described by Alavi and colleagues [28, 37, 38]. Wild type (*Opa1*$^{+/+}$) littermates were systematically used as controls. Upon sacrifice, the brains cortices and livers were dissected out. Tissues were immediately snap frozen in liquid nitrogen and stored at –80ºC.

2.2. Immunoblot Analysis

The brain cortices or livers were thawed on ice. Samples of 20 mg were lysed for 30 min in a buffer containing 50 mM Tris-HCl pH 7.5, 250 mM NaCl, 5 mM ethylenediaminetetraacetic acid (EDTA), 5 mM ethylenebis(oxyethylenenitrilo)tetraacetic acid (EGTA), 1 mM dithiothreitol, 0.1 % Triton X-100, 0.1% SDS, 1% deoxycholate, 1% Tergitol-type NP-40, and protease inhibitors (Complete protease inhibitor mixture, Roche Applied Science, Penzberg, Germany). Lysates were submitted to Dounce homogenization followed by sonication. Cell lysates were then centrifuged at 14,000 *g* at 4°C for 10 min.

Total protein concentration was determined in the supernatant using the Bradford protein assay kit (Bio-Rad, Hercules, CA, USA). 100–200 µg proteins were separated by SDS-PAGE (8–15%) and transferred onto nitrocellulose membranes (Whatman, Protran). Non-specific binding sites were blocked with 5 % non-fat dry milk, 0.2 % Tween 20 in Tris buffer saline pH 7.6 (blocking buffer). The membranes were incubated with the following primary antibodies: anti-OPA1 (1/300, BD-Biosciences, Franklin Lake, NJ, USA), anti-actin (1/25,000, Chemicon/Millipore, Burlington, MA, USA), anti-SOD1 and anti-SOD2 (1/2000, Epitomics, Burlington, MA, USA), anti-catalase (1/3000, Abcam, Burlington, MA, USA), overnight at 4°C in blocking buffer. After chemiluminescent detection of horseradish peroxidase-conjugated secondary antibody (1/10,000, Abcam), scanned photographic films were quantitatively analyzed using ImageJ software (NIH, Bethesda, USA).

2.3. Measurement of Aconitase and Catalase Activities

Measurement of aconitase activities was performed using a protocol described before [39], on 20 mg-samples per replicate. The photochrome was measured at 525 nm using a V630 spectrophotometer (Jasco, Easton, MD, USA). Catalase activity was determined by measuring decomposition of H_2O_2 at 240 nm as described before [40].

2.4. Statistical Analysis

Results are expressed as mean ± standard error of the mean (SEM). Statistical significance was determined by Student's unpaired t test with Welch's correction or followed by a nonparametric post-test (Mann–Whitney). A p value < 0.05 is considered statistically significant.

3. RESULTS

3.1. OPA1 Expression in the Cortices of DOA Mice

We analyzed by immunoblotting the expression of OPA1 in the two *Opa1*$^{+/-}$ and *Opa1*$^{+/+}$ littermate mouse groups. As expected, a decrease in OPA1 lev-

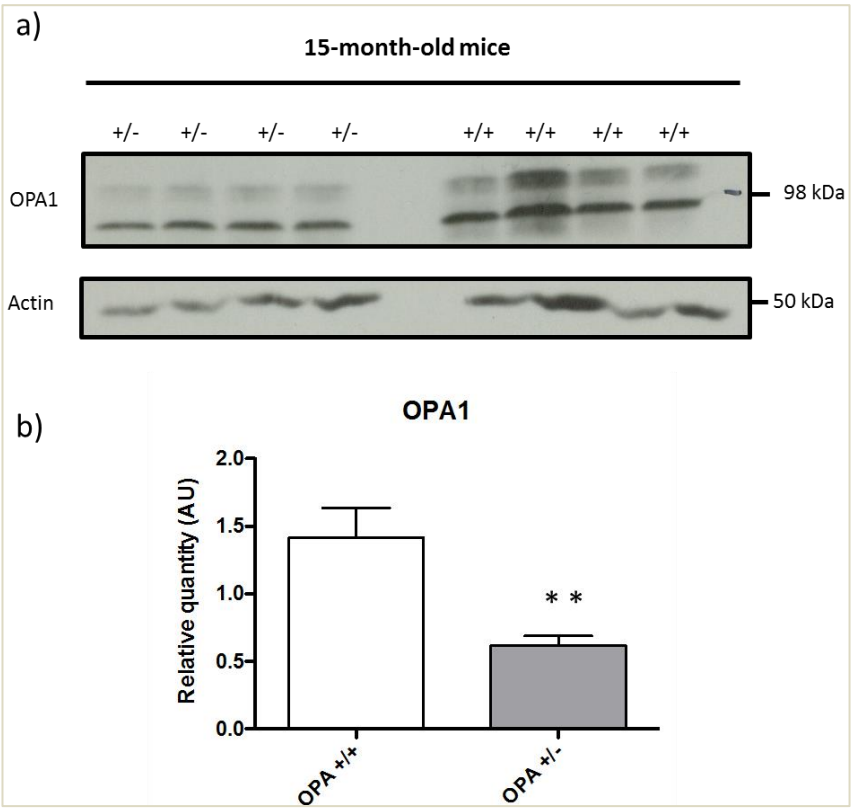

FIGURE 1. OPA1 is down-regulated in the brain cortices of 15-month-old DOA mice. Panel (a): representative immunoblots showing OPA1 and actin protein levels in brain cortices from *Opa1*$^{+/+}$ and *Opa1*$^{+/-}$ mice. Panel (b): quantitative analysis of OPA1 protein levels relative to actin in brain cortices from *Opa1*$^{+/-}$ (white bars, n=9) and *Opa1*$^{+/-}$ (grey bars, n=9) mice. Results are expressed as mean ± SEM. Statistical significance was determined by Student's unpaired t test with Welch's correction, **, $p < 0.01$.

els was evidenced in the cortices of OPA1$^{+/-}$ transgenic mice compared to their *Opa1*$^{+/+}$ littermates (**Figure 1A**). OPA1 appears as several bands as it is the result of the expression of 8 different mRNAs, and in terms of proteins, each splice variant can be processed by one to three proteolytic cleavages generating long and short isoforms [41]. This decrease is about 60% in the brain tissue of *Opa1*$^{+/-}$ mice comparing to *Opa1*$^{+/+}$ littermates.

3.2. Aconitase Activity in the Cortices of DOA Mice

The ROS content of brain cortices from 15-month-old DOA mice was analyzed by monitoring aconitase activity (**Figure 2**). Aconitase was indeed shown to be highly sensitive to oxidation due to damaged iron-sulfur (Fe-S) cluster, and inhibition of its activity is routinely used as a signature of increased mitochondrial ROS production [42–44]. Results demonstrated a significant decrease of aconitase activity, as previously shown in 4- or 10-month-old DOA mice [36]. Such a decrease in aconitase activity strongly supports a higher mitochondrial ROS production in brain cortices of 15-month-old *Opa1*$^{+/-}$ mice.

3.3. Antioxidant Defenses in the Cortices of DOA Mice

Antioxidant defenses induction was monitored as a consequence of increased ROS levels. The protein levels of superoxide dismutases 1 and 2 (SOD1 and

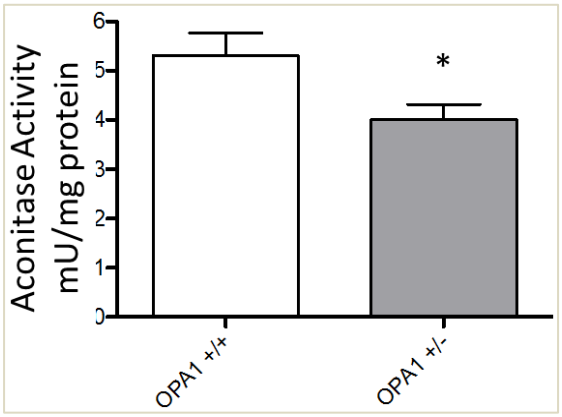

FIGURE 2. Aconitase activity is reduced in the brain cortices of 15-month-old DOA mice. Aconitase activity was measured in the cortices of *Opa1*$^{+/+}$ (white bars, n = 7) and *Opa1*$^{+/-}$ (grey bars, n = 7) littermate mice. Results are expressed as mean ± SEM. Statistical significance was determined by Student's unpaired t-test followed by a nonparametric post-test (Mann-Whitney), *, $p < 0.05$.

SOD2), that catalyze the dismutation of superoxide anion into hydrogen peroxide, and of the detoxifying catalase, that catalyzes the transformation of hydrogen peroxide into water and oxygen, were estimated by immunoblotting in the brain cortices extracts from 15-month-old *Opa1*$^{+/-}$ mice and wild-type littermates (**Figure 3**). Data reveal that neither SOD1 nor SOD2 nor catalase protein levels are changed in the brain cortices from *Opa1*$^{+/-}$ mice when compared to wild-type littermates at 15 months of age. Similarly, no change in catalase activity was observed in the cortices of both *Opa1*$^{+/-}$ and *Opa1*$^{+/+}$ mice (**Figure 4**). As a comparison, analyses of the quantities of SOD1, SOD2 and catalase protein levels in the livers from the same mice at 4 and 15 months of age showed no significant difference (data not shown). Thus, altogether, these data reinforce the notion that the brain cortices of 15-month-old *Opa1*$^{+/-}$ mice are in a pro-oxidative state.

4. DISCUSSION

A decrease in aconitase activity, as observed here, strongly supports a higher mitochondrial ROS production in the brains of aged *Opa1*$^{+/-}$ mice as compared to wild-type littermates. Aconitase activity is used as a marker of increased mitochondrial ROS production because of the susceptibility of this enzyme to oxidation due to damaged Fe-S cluster [42–44]. Our team previously showed that down-regulation of OPA1 correlated with a significant inhibition of aconitase activity in both 4- and 10-month-old *Opa1*$^{+/-}$ transgenic mice compared with their wild-type littermates, as well as in OPA1-deleted neurons in primary culture [36]. Thus, in an OPA1-deficient context, aging is correlated with a persistent higher mitochondrial ROS production in the mouse brain.

Similarly, the herein measured levels of detoxifying enzymes like SOD1, SOD2, and catalase do not differ in the brain cortices of 15-month-old *Opa1*$^{+/-}$ mice compared to control ones, and neither was catalase activity. This is in line with our previous results on brain cortices from younger DOA mice which displayed similar protein levels in both genotypes regardless of age but displayed a strong 2-fold increase in both SOD1 and SOD2 from 4 to 10 months of age. Thus, after 15 months, the brains of *Opa1*$^{+/-}$ mice are still in a pro-oxidative state.

Interestingly, such age-dependent pro-oxidative stress can be related to the evolution of the disease since *Opa1*$^{+/-}$ mice experience a worsening of their vision after 13 months [28]. Moreover, re-evaluation of a cohort of DOA patients a few years ago demonstrated that more than 20 % of DOA patients develop a DOA plus syndrome (for review, see [45]).

The extraocular features of the DOA+ syndrome can include sensorineural deafness, ataxia, myopathy, chronic progressive external ophthalmoplegia, and peripheral neuropathy. But, other rare associations of OPA1 mutations have been reported in adults with spastic paraplegia [14], the multiple sclerosis-like syndrome [10], the Behr-like syndrome [46], and, more recently, with syndromic parkinsonism and dementia [47]. The pro-oxidative state in old *Opa1*$^{+/-}$ mice would be one of the keys encountered in patients suffering from the DOA+ syndrome, and more generally confirms that OPA haploinsufficiency leads to a pro-oxidative state.

As mentioned in the Introduction section, there is a marked inter- and intra-familial difference in terms of severity of DOA and other diseases related to *OPA1* gene disorders. In this context, our perspective is to build up a mathematical model of the molecular

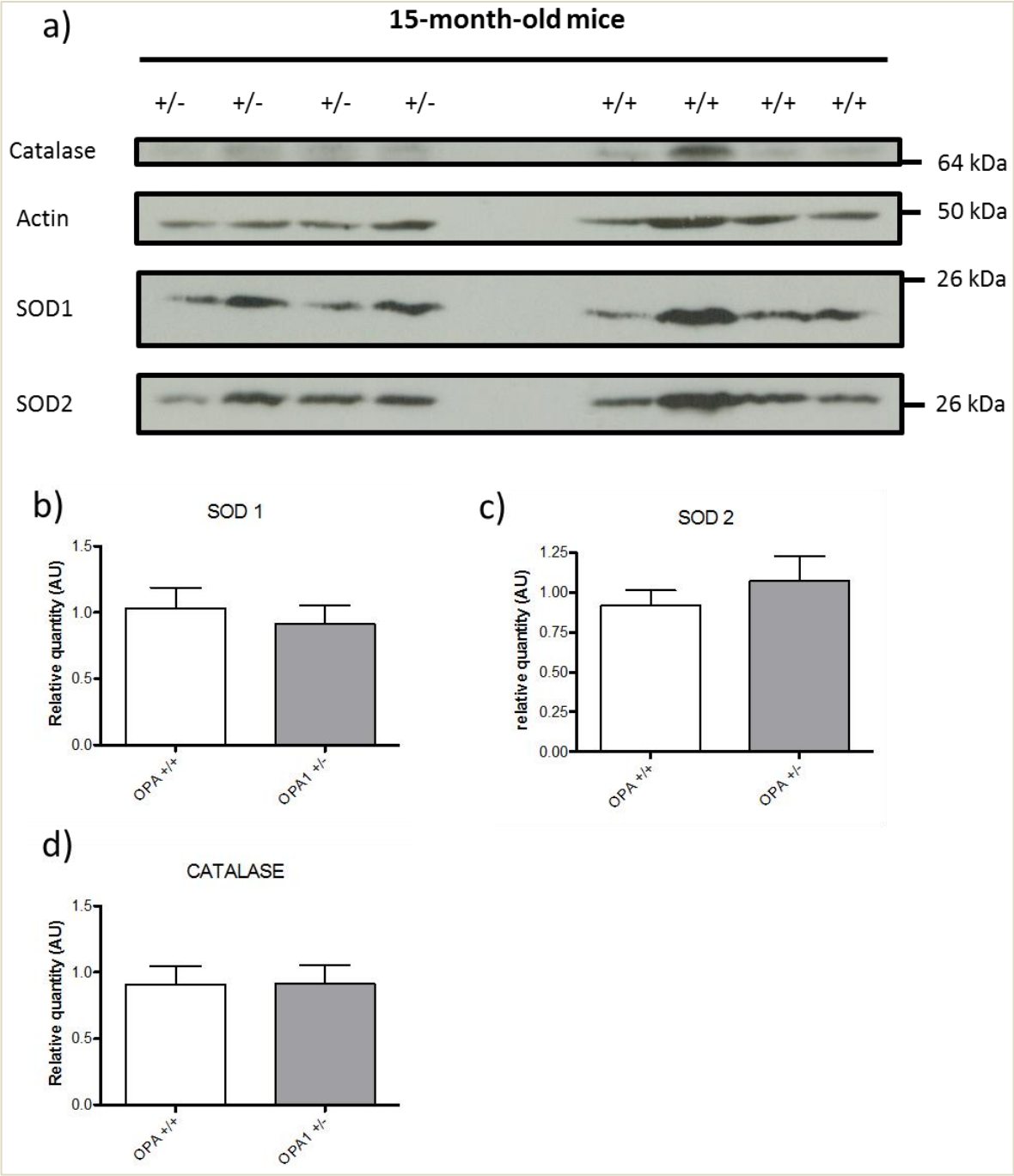

FIGURE 3. Redox state is imbalanced in the brain cortices of 15-month-old DOA mice. Panel (a): representative immunoblots showing SOD1, SOD2, catalase, and actin protein levels in the cortices of 15-month-old *Opa1*$^{+/+}$ and *Opa1*$^{+/-}$ littermate mice. Panels (b), (c), and (d): histograms representative of SOD1 (b), SOD2 (c), and catalase (d) protein quantities in the cortices of 15-month-old *OPA*$^{+/+}$ (white bars, n = 9) and *Opa1*$^{+/-}$ mice (grey bars, n = 9). Results are expressed as mean ± SEM. Statistical significance was determined by Student's unpaired t test with Welch's correction.

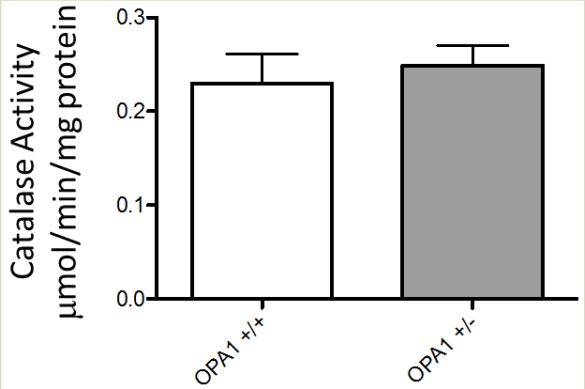

FIGURE 4. Catalase activity is unchanged in the brain cortices of 15-month-old DOA mice. Histograms represent catalase activity estimated in *Opa1*$^{+/+}$ (white bars, n = 9) and *Opa1*$^{+/-}$ (grey bars, n = 9) littermate mice cortices. Results are expressed as mean ± SEM. Statistical significance was determined by Student's unpaired t-test followed by a nonparametric post-test (Mann-Whitney), *, $p < 0.05$.

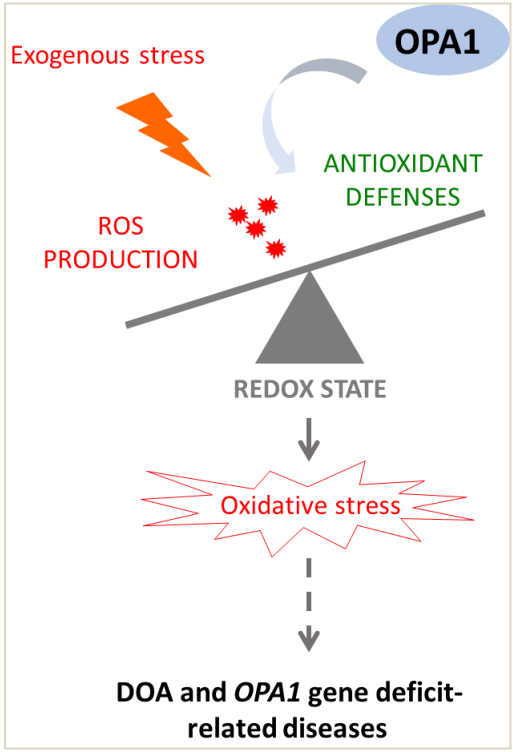

FIGURE 5. Cascade of events modifying the oxidative metabolism in DOA and *OPA1* gene deficit-related diseases. This scheme was adopted from Ref. [49].

mechanisms involved in DOA pathogenesis in order to predict the evolution of the disease in patients. Such a model would allow determining the appropriate treatment based on in-silico analysis fueled with physiological parameters specific for each patient. In order to obtain an algorithm able to predict ROS production and detoxification by antioxidant defenses, a stochastic model of catalytic activity and ROS production of the complex I of the mitochondrial respiratory chain was characterized. So far, our model is able to reproduce the dynamics of the complex I system and to simulate the observed behaviors of this system regarding ROS production [48, 49]. Fueled with our in vivo data, this first step towards a bigger model involving ROS production and antioxidant defenses paves the way for predictive medicine (**Figure 5**).

ACKNOWLEDGMENTS

This project was supported by grants from the Centre National de la Recherche Scientifique, the Université Paul Sabatier, Rétina-France, the Union Nationale Des Aveugles et Déficients Visuels, the Gueules Cassées Sourire quand même, the Association contre les Maladies Mitochondriales, and the Region Occitanie. Regarding author contributions, N.D. conceived and designed the experiments; M.D., A.M., and V.M. performed the experiments; N.D. and P.B. analyzed the data; B.W. contributed with the mice; N.D. and M-C. M. wrote the paper. The authors of the paper declare no conflicts of interest. The funding sponsors had no role in the design of the study; in the collection, analyses, or interpretation of data; in the writing of the manuscript; and in the decision to publish the results. Regarding patents, the international N PCT/EP2015/056814 is resulting from the work reported in this manuscript.

REFERENCES

1. Osellame LD, Blacker TS, Duchen MR. Cellular

and molecular mechanisms of mitochondrial function. *Best Pract Res Clin Endocrinol Metab* 2012; 26(6):711–23. doi: 10.1016/j.beem.2012.05.003.
2. Koopman WJ, Distelmaier F, Smeitink JA, Willems PH. OXPHOS mutations and neurodegeneration. *EMBO J* 2013; 32(1):9–29. doi: 10.1038/emboj.2012.300.
3. Carelli V, La Morgia C, Valentino ML, Barboni P, Ross-Cisneros FN, Sadun AA. Retinal ganglion cell neurodegeneration in mitochondrial inherited disorders. *Biochim Biophys Acta* 2009; 1787(5):518–28. doi: 10.1016/j.bbabio.2009.02.024.
4. Amati-Bonneau P, Milea D, Bonneau D, Chevrollier A, Ferre M, Guillet V, et al. OPA1-associated disorders: phenotypes and pathophysiology. *Int J Biochem Cell Biol* 2009; 41(10):1855–65. doi: 10.1016/j.biocel.2009.04.012.
5. Yu-Wai-Man P, Trenell MI, Hollingsworth KG, Griffiths PG, Chinnery PF. OPA1 mutations impair mitochondrial function in both pure and complicated dominant optic atrophy. *Brain* 2011; 134(Pt 4):e164. doi: 10.1093/brain/awq288.
6. Lenaers G, Hamel C, Delettre C, Amati-Bonneau P, Procaccio V, Bonneau D, et al. Dominant optic atrophy. *Orphanet J Rare Dis* 2012; 7:46. doi: 10.1186/1750-1172-7-46.
7. Delettre C, Lenaers G, Griffoin JM, Gigarel N, Lorenzo C, Belenguer P, et al. Nuclear gene OPA1, encoding a mitochondrial dynamin-related protein, is mutated in dominant optic atrophy. *Nat Genet* 2000; 26(2):207–10.
8. Alexander C, Votruba M, Pesch UE, Thiselton DL, Mayer S, Moore A, et al. OPA1, encoding a dynamin-related GTPase, is mutated in autosomal dominant optic atrophy linked to chromosome 3q28. *Nat Genet* 2000; 26(2):211–5.
9. Cohn AC, Toomes C, Potter C, Towns KV, Hewitt AW, Inglehearn CF, et al. Autosomal dominant optic atrophy: penetrance and expressivity in patients with OPA1 mutations. *Am J Ophthalmol* 2007; 143(4):656–62.
10. Yu-Wai-Man P, Griffiths PG, Burke A, Sellar PW, Clarke MP, Gnanaraj L, et al. The prevalence and natural history of dominant optic atrophy due to OPA1 mutations. *Ophthalmology* 2010; 117(8):1538–46, 46 e1. doi: 10.1016/j.ophtha.2009.12.038.
11. Amati-Bonneau P, Valentino ML, Reynier P, Gallardo ME, Bornstein B, Boissiere A, et al. OPA1 mutations induce mitochondrial DNA instability and optic atrophy 'plus' phenotypes. *Brain* 2008; 131(Pt 2):338–51.
12. Hudson G, Amati-Bonneau P, Blakely EL, Stewart JD, He L, Schaefer AM, et al. Mutation of OPA1 causes dominant optic atrophy with external ophthalmoplegia, ataxia, deafness and multiple mitochondrial DNA deletions: a novel disorder of mtDNA maintenance. *Brain* 2008; 131(Pt 2):329–37.
13. Zeviani M. OPA1 mutations and mitochondrial DNA damage: keeping the magic circle in shape. *Brain* 2008; 131(Pt 2):314–7. doi: 10.1093/brain/awm339.
14. Yu-Wai-Man P, Griffiths PG, Gorman GS, Lourenco CM, Wright AF, Auer-Grumbach M, et al. Multi-system neurological disease is common in patients with OPA1 mutations. *Brain* 2010; 133(Pt 3):771–86. doi: 10.1093/brain/awq007.
15. Spinazzi M, Cazzola S, Bortolozzi M, Baracca A, Loro E, Casarin A, et al. A novel deletion in the GTPase domain of OPA1 causes defects in mitochondrial morphology and distribution, but not in function. *Hum Mol Genet* 2008; 17(21):3291–302.
16. Mackey DA, Trounce I. Genetics: Optic nerve genetics: more than meets the eye. *Nat Rev Neurol* 2010; 6(7):357–8. doi: 10.1038/nrneurol.2010.77.
17. Olichon A, Emorine LJ, Descoins E, Pelloquin L, Brichese L, Gas N, et al. The human dynamin-related protein OPA1 is anchored to the mitochondrial inner membrane facing the inter-membrane space. *FEBS Lett* 2002; 523(1–3):171–6.
18. Griparic L, van der Wel NN, Orozco IJ, Peters PJ, van der Bliek AM. Loss of the intermembrane space protein Mgm1/OPA1 induces swelling and localized constrictions along the lengths of mitochondria. *J Biol Chem* 2004; 279(18):18792–8. doi: 10.1074/jbc.M400920200.
19. Satoh M, Hamamoto T, Seo N, Kagawa Y, Endo H. Differential sublocalization of the dynamin-related protein OPA1 isoforms in mitochondria. *Biochem Biophys Res Commun* 2003;

300(2):482–93.
20. Ishihara N, Fujita Y, Oka T, Mihara K. Regulation of mitochondrial morphology through proteolytic cleavage of OPA1. *EMBO J* 2006; 25(13):2966–77. doi: 10.1038/sj.emboj.7601184.
21. Belenguer P, Pellegrini L. The dynamin GTPase OPA1: more than mitochondria? *Biochim Biophys Acta* 2013; 1833(1):176–83. doi: 10.1016/j.bbamcr.2012.08.004.
22. Olichon A, Baricault L, Gas N, Guillou E, Valette A, Belenguer P, et al. Loss of OPA1 perturbates the mitochondrial inner membrane structure and integrity, leading to cytochrome c release and apoptosis. *J Biol Chem* 2003; 278(10):7743–6.
23. Elachouri G, Vidoni S, Zanna C, Pattyn A, Boukhaddaoui H, Gaget K, et al. OPA1 links human mitochondrial genome maintenance to mtDNA replication and distribution. *Genome Res* 2011; 21(1):12–20. doi: 10.1101/gr.108696.110.
24. Frezza C, Cipolat S, Martins de Brito O, Micaroni M, Beznoussenko GV, Rudka T, et al. OPA1 controls apoptotic cristae remodeling independently from mitochondrial fusion. *Cell* 2006; 126(1):177–89. doi: 10.1016/j.cell.2006.06.025.
25. Zanna C, Ghelli A, Porcelli AM, Karbowski M, Youle RJ, Schimpf S, et al. OPA1 mutations associated with dominant optic atrophy impair oxidative phosphorylation and mitochondrial fusion. *Brain* 2008; 131(Pt 2):352–67.
26. Lodi R, Tonon C, Valentino ML, Manners D, Testa C, Malucelli E, et al. Defective mitochondrial adenosine triphosphate production in skeletal muscle from patients with dominant optic atrophy due to OPA1 mutations. *Arch Neurol* 2011.
27. Davies VJ, Hollins AJ, Piechota MJ, Yip W, Davies JR, White KE, et al. Opa1 deficiency in a mouse model of autosomal dominant optic atrophy impairs mitochondrial morphology, optic nerve structure and visual function. *Hum Mol Genet* 2007; 16(11):1307–18. doi: 10.1093/hmg/ddm079.
28. Alavi MV, Bette S, Schimpf S, Schuettauf F, Schraermeyer U, Wehrl HF, et al. A splice site mutation in the murine Opa1 gene features pathology of autosomal dominant optic atrophy. *Brain* 2007; 130(Pt 4):1029–42. doi: 10.1093/brain/awm005.
29. Sarzi E, Angebault C, Seveno M, Gueguen N, Chaix B, Bielicki G, et al. The human OPA1delTTAG mutation induces premature age-related systemic neurodegeneration in mouse. *Brain* 2012; 135(Pt 12):3599–613. doi: 10.1093/brain/aws303.
30. Kanazawa T, Zappaterra MD, Hasegawa A, Wright AP, Newman-Smith ED, Buttle KF, et al. The C. elegans Opa1 homologue EAT-3 is essential for resistance to free radicals. *PLoS Genet* 2008; 4(2):e1000022.
31. Yarosh W, Monserrate J, Tong JJ, Tse S, Le PK, Nguyen K, et al. The molecular mechanisms of OPA1-mediated optic atrophy in Drosophila model and prospects for antioxidant treatment. *PLoS Genet* 2008; 4(1):e6.
32. Tang S, Le PK, Tse S, Wallace DC, Huang T. Heterozygous mutation of Opa1 in Drosophila shortens lifespan mediated through increased reactive oxygen species production. *PLoS One* 2009; 4(2):e4492.
33. Shahrestani P, Leung HT, Le PK, Pak WL, Tse S, Ocorr K, et al. Heterozygous mutation of Drosophila Opa1 causes the development of multiple organ abnormalities in an age-dependent and organ-specific manner. *PLoS One* 2009; 4(8):e6867. doi: 10.1371/journal.pone.0006867.
34. Yen MY, Wang AG, Wei YH. Leber's hereditary optic neuropathy: a multifactorial disease. *Prog Retin Eye Res* 2006; 25(4):381–96. doi: 10.1016/j.preteyeres.2006.05.002.
35. Yan MH, Wang X, Zhu X. Mitochondrial defects and oxidative stress in Alzheimer disease and Parkinson disease. *Free Radic Biol Med* 2013; 62:90–101. doi: 10.1016/j.freeradbiomed.2012.11.014.
36. Millet AM, Bertholet AM, Daloyau M, Reynier P, Galinier A, Devin A, et al. Loss of functional OPA1 unbalances redox state: implications in dominant optic atrophy pathogenesis. *Ann Clin Transl Neurol* 2016; 3(6):408–21. doi: 10.1002/acn3.305.
37. Alavi MV, Fuhrmann N, Nguyen HP, Yu-Wai-Man P, Heiduschka P, Chinnery PF, et al. Subtle neurological and metabolic abnormalities in an Opa1 mouse model of autosomal dominant optic atrophy. *Exp Neurol* 2009; 220(2):404–9. doi:

10.1016/j.expneurol.2009.09.026.
38. Heiduschka P, Schnichels S, Fuhrmann N, Hofmeister S, Schraermeyer U, Wissinger B, et al. Electrophysiological and histologic assessment of retinal ganglion cell fate in a mouse model for OPA1-associated autosomal dominant optic atrophy. *Invest Ophthalmol Vis Sci* 2010; 51(3):1424–31. doi: 10.1167/iovs.09-3606.
39. Colombani AL, Carneiro L, Benani A, Galinier A, Jaillard T, Duparc T, et al. Enhanced hypothalamic glucose sensing in obesity: alteration of redox signaling. *Diabetes* 2009; 58(10):2189–97. doi: 10.2337/db09-0110.
40. Galinier A, Carriere A, Fernandez Y, Carpene C, Andre M, Caspar-Bauguil S, et al. Adipose tissue proadipogenic redox changes in obesity. *J Biol Chem* 2006; 281(18):12682–7. doi: 10.1074/jbc.M506949200.
41. Song Z, Chen H, Fiket M, Alexander C, Chan DC. OPA1 processing controls mitochondrial fusion and is regulated by mRNA splicing, membrane potential, and Yme1L. *J Cell Biol* 2007; 178(5):749–55. doi: 10.1083/jcb.200704110.
42. Vincent AM, McLean LL, Backus C, Feldman EL. Short-term hyperglycemia produces oxidative damage and apoptosis in neurons. *FASEB J* 2005; 19(6):638–40. doi: 10.1096/fj.04-2513fje.
43. Gardner PR, Nguyen DD, White CW. Aconitase is a sensitive and critical target of oxygen poisoning in cultured mammalian cells and in rat lungs. *Proc Natl Acad Sci USA* 1994; 91(25):12248–52.
44. Kelly M, Trudel S, Brouillard F, Bouillaud F, Colas J, Nguyen-Khoa T, et al. Cystic fibrosis transmembrane regulator inhibitors CFTR(inh)-172 and GlyH-101 target mitochondrial functions, independently of chloride channel inhibition. *J Pharmacol Exp Ther* 2010; 333(1):60–9. doi: 10.1124/jpet.109.162032.
45. Chao de la Barca JM, Prunier-Mirebeau D, Amati-Bonneau P, Ferre M, Sarzi E, Bris C, et al. OPA1-related disorders: diversity of clinical expression, modes of inheritance and pathophysiology. *Neurobiol Dis* 2016; 90:20–6. doi: 10.1016/j.nbd.2015.08.015.
46. Marelli C, Amati-Bonneau P, Reynier P, Layet V, Layet A, Stevanin G, et al. Heterozygous OPA1 mutations in Behr syndrome. *Brain* 2011; 134(Pt 4):e169; author reply e70. doi: 10.1093/brain/awq306.
47. Carelli V, Musumeci O, Caporali L, Zanna C, La Morgia C, Del Dotto V, et al. Syndromic parkinsonism and dementia associated with OPA1 missense mutations. *Ann Neurol* 2015; 78(1):21–38. doi: 10.1002/ana.24410.
48. Merabet N, Bordeneuve-Guibe J, Davezac N. Modelling the redox imbalance in dominant optic atrophy: the case of respiratory complex I. *IFAC-PapersOnLine* 2017; 50.
49. Millet A. MN, Bertholet A., Daloyau M.,, Reynier P. GA, Devin A., Wissinger B.,, Bordeneuve-guibe J. BP, Davezac N. Imbalance of the REDOX state in dominant Optic Atrophy: the way of mathematical modeling. *Arch Int Soc Antioxid iNutri Health* 2017; 5(1):21–4.